sciendo

Research on energy absorption properties of open-cell copper foam for current collector of Li-ions

JIAN CHEN, XIONGFEI LI, WEI LI*, CONG LI, BAOSHAN XIE, SHUOWEI DAI, JIAN-JUN HE, YANJIE REN

School of Energy and Power Engineering, Changsha University of Science and Technology, Changsha, Hunan, 410004, China

Quasi-static uniaxial compressive tests of open-cell copper (Cu) foams (OCCF) were carried out on an in-situ bi-direction tension/compress testing machine (IBTC 2000). The effects of strain rate, porosity and pore size on the energy absorption of open-cell copper foams were investigated to reveal the energy absorption mechanism. The results show that three performance parameters of open-cell copper foams (OCCF), involving compressive strength, Young modulus and yield stress, increase simultaneously with an increase of strain rate and reduce with increasing porosity and pore size. Furthermore, the energy absorption capacity of OCCF increases with an increase of porosity and pore size. However, energy absorption efficiency increases with increasing porosity and decreasing pore size. The finite element simulation results show that the two-dimensional stochastic model can predict the energy absorption performance of the foam during the compressive process. The large permanent plastic deformation at the weak edge hole is the main factor that affects the energy absorption.

Keywords: *open-cell copper foam; true stress-strain curve; energy absorption; finite element simulation*

1. Introduction

Lithium-ion secondary battery (Li-ion) has a large-scale applications in engineering and scientific field because of its high energy efficiency, which has a great meaning for portable electronic devices. Its energy and power density, cycle life and safety have to be improved for cell-driven vehicles, aerospace engineering, military industry and large-scale energy storage systems. Currently, graphite, which is coated on the surface of the copper foil current collector, is adopted as a negative electrode material of Li-ion batteries. However, the electrode volume may change because of the activity of lithium intercalation/deintercalation during charge and discharge processes [1]. The volume change may lead to the structure failure of active material and the separation of electrode material and current collector. The electrode capacity will decay and eventually the electrode may even fail [2–14]. The tremendous volume change of the negative electrode material with a high storage capacity during the charging and discharging process

of lithium-ion battery is the bottleneck for the applications of electrode materials.

To eliminate the volume change caused by the intercalation/deintercalation, the open-cell copper foam was proposed to be used as a negative collector material for its porous cellular structure and excellent performance. As a lithium-ion battery electrode material, collector which is a channel for internal and external electrons transmission, can be subjected to a compressive load under actual operating conditions. Furthermore, the energy change caused by volume expansion when lithium is intercalated into negative material can be buffered and adjusted by compressive deformation of OCCF. Therefore, the storage capacity and safety of Li-ion batteries is improved [15]. Ke et al. [16–18] prepared electrode materials of Sn–Cu, Sn–Co or Sn–Ni with a high porosity using electrodeposition. It was found that this material had a superior cycle performance of high-density kayserzinn electrode material. Besides that, Shin and Liu [19], Mastragostino et al. [20] and Zhao et al. [21] investigated the electrochemical properties of three-dimensional porous Cu–Sn alloy. It was found that the porous structure of the samples contributed

---

*E-mail: zzgjiajie1128@126.com

to the improvement of cycle performance. However, its instability caused microcracks on the surface of the porous Cu_6Sn_5 alloy electrode, resulting in a decreasing storage capacity during the latter stage of cycling. Ionica et al. [22] observed that rod-like Cu nanostructures of Ni_3Sn_4 metallic compound can be grown on these 3-D structures for weakening the volume changes of electrode so that the electrode was able to maintain its stability under a cycle rate of 500 mA h/g, and also performance degradations after 200 times cycles did not appear. According to previous studies in which copper foams and porous copper alloy materials were used as negative electrode materials or current collector, it can be found that electrochemical performance of electrode material is the priority of research. Because of the open-cell foams with an excellent compressive characteristics, they are regarded as appropriate negative current collector material. The energy variation caused by volume expansion could be buffered and adjusted in Li^+ intercalation process. In addition, the storage capacity could be enhanced. The energy absorption mechanism of the foam materials focuses on aluminum foam currently. Qin et al. [23] analyzed energy absorbtion of aluminum foams under impulsive load using mesoscopic model. It was concluded that the absorptive capacity was prominently related to the loading rate and strength of hole-wall. Macroscopic analysis showed that the plastic strain and fracture of the pore wall were the origin of energy absorption of the aluminum foam. A. Jung et al. [24] investigated the energy absorption properties of open-cell aluminum foams covered with nickel or uncoated nickel and found that aluminum foam partially or gradually covering with nickel had a promising capability to absorb energy at a wide range of loading rates. Sun et al. [25] investigated the mechanical properties of such Al/Cu hybrid foam. This method improved the ductility of Al/Cu hybrid foam and effectively enhanced the energy absorption capacity of open-cell foam. Rajak et al. [26] studied the compressive behavior of the strain rate between 10^{-1}/s and about 10^{-3}/s and found that the energy absorption performance of the aluminum foam increased with the stress of the platform. The lower density foam

could absorb a large amount of energy. However, the energy absorption of OCCF is seldom. There are still several major issues and questions like how to analyze the impact of porous structure on energy absorption efficiency from the standpoint of the mechanism.

This paper experimentally analyzes the mechanical properties of OCCF. The tests were conducted under different strain rates by using an *in-situ* bi-direction tension/compress testing machine (IBTC 2000). The effect of strain rate, porosity and pore size on the energy absorption efficiency of OCCF have been analyzed. Finite element analysis method has been used to analyze the energy absorption mechanism.

2. Experimental

2.1. Specimen preparation

In this study open-cell copper foams (OCCF) with the PPI (pores per inch, 1 in. = 25.4 mm) of 5, 20, 30 and porosity of about 90.3 % to approximately 96.4 % were prepared. Five kinds of materials with different pore sizes and porosities were cut into 24 mm × 30 mm cylindrical specimens by wire cut electrical discharge machining (WEDM). The samples were weighed with an electronic weight, the porosity P and the relative density ρ_R of the samples were obtained according to equation 1 and equation 2 [25]:

$$P = 1 - \frac{4m}{\pi \rho h \varnothing^2} \qquad (1)$$

$$\rho_R = 1 - P \qquad (2)$$

where m, h, Φ are the standard sample of copper foam quality, height and diameter of the bottom circle, respectively; ρ is the density of pure copper. The characteristic parameters of the open-cell copper foam used in the experiments are collected in Table 1. The optical micrograph for 3-D structure of specimen #2 is shown in Fig. 1.

2.2. OCCF specimens testing

The compressive tests on OCCFs were conducted at different strain rates of 10^{-2}/s, 10^{-3}/s,

Table 1. Porosity and PPI values of the open-cell copper foams.

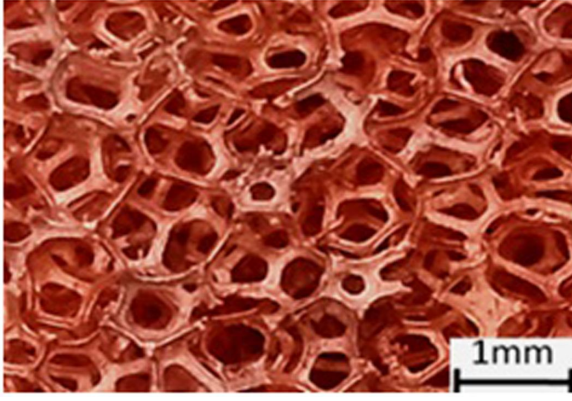| No.	Porosity [%]	PPI	Relative densities
1#	95.7	30	0.043
2#	96.4	20	0.036
3#	90.3	5	0.097
4#	92.5	5	0.080
5#	95.8	5	0.042

Fig. 1. Optical micrograph of open-cell copper foam.

and 10^{-4}/s using an *in-situ* bi-direction tension/compress testing machine to obtain the OCCFs' compressive performance. In the testing process, the cross-head and specimens were lubricated using vaseline to minimize the friction coefficient between these two parts. Instantaneous displacement and analytical data were obtained. True stress-strain curves based on porosity and pore size were drawn based on the experimental data.

3. Results and discussions

3.1. Analysis of true stress-strain curves

In Fig. 2a, the typical true stress-strain curves of the quasi-static compressive test for five OCCF specimens are presented. The specimens of different porosities and pore sizes were tested under different strain rates. It clearly shown that the stress-strain curves of copper foam at different strain rates comprise three stages: elastic stage, plastic stage

and densification stage. The compressive behavior of OCCFs under quasi-static loading is presented in Fig. 2b.

In elastic stage, the deformation is caused by the pore struts. A linear relationship between stress and strain is observed. The value of strain is less than or equal to 0.05 ($\epsilon \leqslant 0.05$). There is almost no change of the pore shape at the strain of 3 %, as shown in Fig. 2b. Moreover, Young modulus as well as the pore size and porosity decrease as the strain rate increases. When stress increases, pore-struts cause the further deformation. Irreversible deformation occurs when the stress reaches the yield strength of copper foam. The deformation comes to the plastic stage. At this stage, a higher porosity and larger size of pore lead to a decrease in compressive strength. In Fig. 2b (true strain of 10 % or 25 %), a random distribution of inclined deformation belt is observed, which is perpendicular to or inclined at an angle of 45°to the loading direction. Most pores gradually collapse in these deformation areas and a few of them collapse completely, which is the feature of failure mechanism of layer by layer collapsing. The collapsed pores merge into a larger horizontal deformation zone (black line marked area) with further compressive load. Increasing the compressive load results in increased densification of the copper foams. That is, the deformation comes to the densification stage. A large amount of mechanical energy is absorbed during the whole deformation process.

3.2. Effect of energy absorption ability on strain rate, porosity and pore size

The response curve of metal foams has a wide range of stress platform region in uniaxial compressive test. The energy absorption ability E_v and efficiency η are expressed as:

$$E_V = \int_0^{\varepsilon_{max}} \sigma d\varepsilon \tag{3}$$

$$\eta = \frac{\int_0^{\varepsilon_{max}} \sigma d\varepsilon}{\varepsilon_{max} \sigma_{max}} \tag{4}$$

where σ and ϵ is compressive stress and strain, ϵ_{max} is the maximum strain, σ_{max} is the maximum
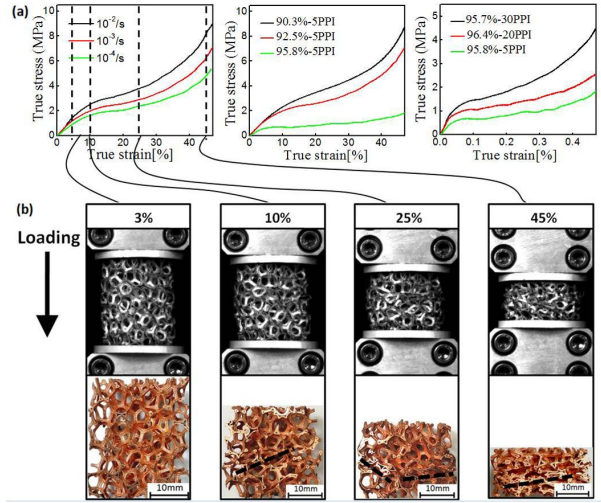
Fig. 2. True stress-strain curves and cross-sections of open-cell copper foam at different strains:(a) 3 %, (b)10 %, (c) 25 % and (d) 45 %.

stress corresponding to maximum strain [27]. Energy absorption ability E_v is equal to areas under true stress-strain curve according to equation 3. And the energy absorption efficiency η is the ratio between a foam material and an ideal plastic material when they are under the same strain. The energy absorption performance depends on energy absorption ability E_v and efficiency η. Obviously, the OCCF absorbs less amount of energy at the elastic stage than the energy that is absorbed at plastic stage. At plastic stage, more energy is required for the plastic deformation of pore-struts. Moreover, the OCCF experiences a small stress variation with a large strain variation, which absorbs a large amount of extrinsic energy. Energy absorption ability is related to the true stress-strain curves. Specifically, porosity and pore size are the critical factors that affect the energy absorption ability.

Fig. 3 and Fig. 4 show the influences of strain rate, porosity and pore size on energy absorption ability and efficiency. When the porosity and pore size are constants, it is found that the high strain rate-curve shifts to upper right region when strain rate increases in Fig. 3, which means that OCCF possesses higher energy absorption ability under high strain loading rate. The curves cross when
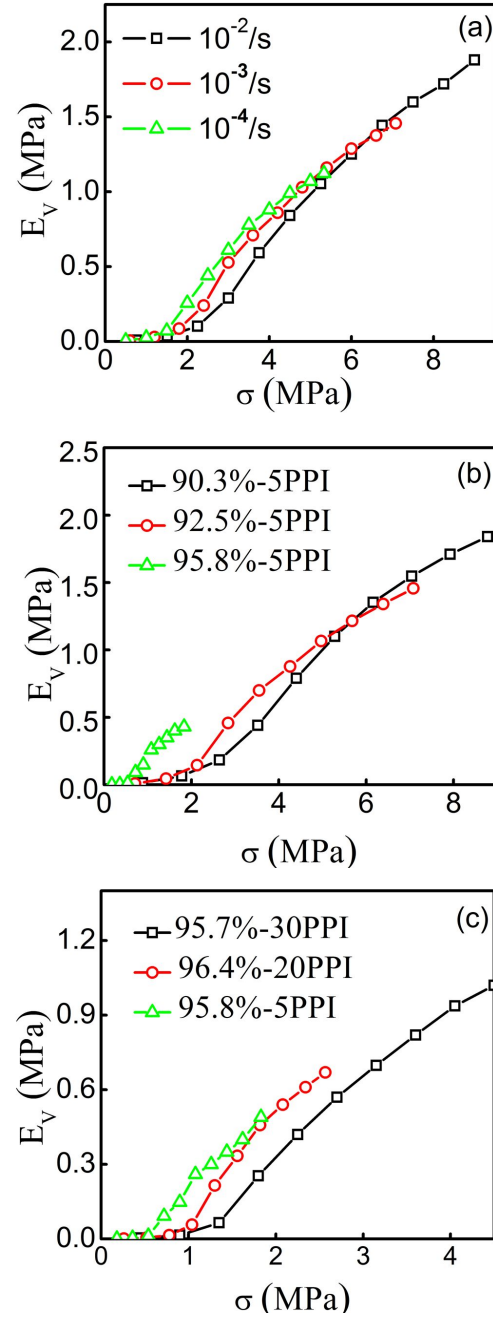

Fig. 3. Factors influencing energy absorption capacity: (a) strain rate, (b) porosity, and (c) pore size.

stress increases to 5 MPa to 7 MPa because of the relatively short platform region. When the strain rate and pore size are constant, it can be observed that the high porosity-curve shifts to upper right region with increasing porosity. That is, the OCCF with a higher porosity possesses stronger energy
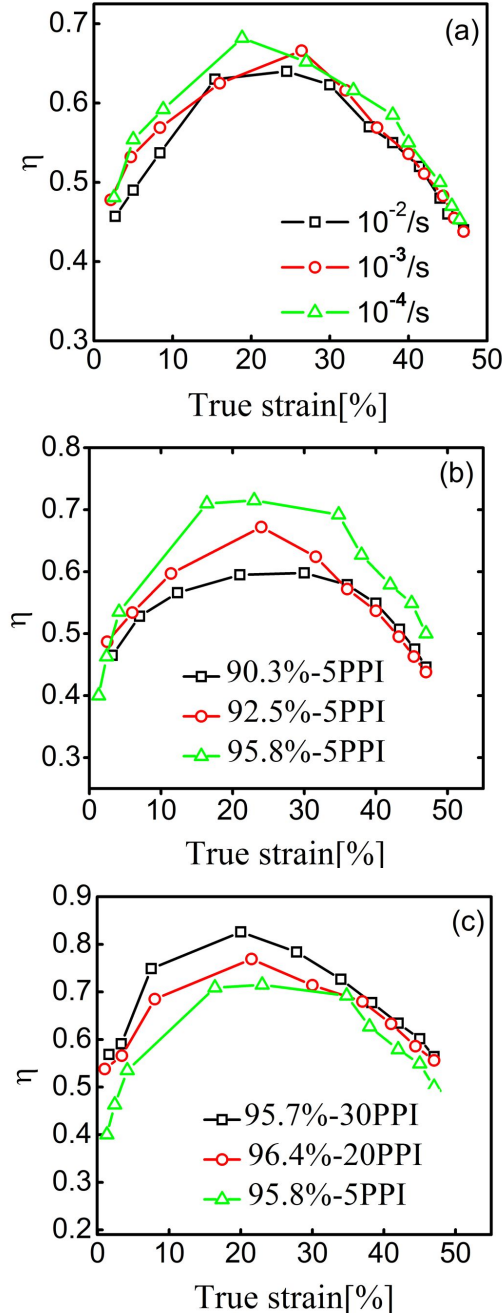
higher than 65 %. The maximum energy absorption efficiency is obtained when the strain is between 20 % and 30 %. Consequently, the energy absorption efficiency increases with increasing porosity, decreasing strain rate and pore size. In summary, increasing porosity, reducing the size of pore as well as decreasing the loading rate will enhance the energy absorption efficiency of OCCF.

3.3. Simulation of OCCFs energy absorption process

In order to reveal the energy absorption mechanism of OCCF with high porosity, the deformation, stress concentration and the local strain under compressive process were simulated using finite element software (ABAQUS). The longitudinal profile of a cylindrical sample was observed by macro-tomography. Using the finite element software ABAQUS, a two-dimensional model with the size of 24 mm × 30 mm was produced to investigate the plastic deformation behavior, stress distribution and the energy absorption behavior under uniaxial compressive loads. The elastic-plastic constitutive model in ABAQUS is employed to simulate the pore-struts and OCCF. The plastic hardening parameters are shown in Table 2. Loading mode of test and simulation is illustrated in Fig. 5. Related parameters are as follows: density $\rho = 8900$ kg/m^3, Young modulus E = 29.83 MPa, Poisson ratio $\mu = 0.32$, friction coefficient = 0.02. In this work, rigid indenter contact with the specimen surface was assumed The pores within the OCCF contacted with each other. Dynamic-Explicit of ABAQUS was adopted to obtain stress-strain curves of the whole and partial specimens.

The OCCF with 5-PPI and a porosity of 92.5 % was used for the simulations to obtain the data for the nephogram of equivalent stress distribution with different strains. The stress distribution along with pores is shown in Fig. 6. The stress along the pore-struts is larger than that along the knots. The original plastic deformation mainly appear at the weak spots of the pore-struts. With increasing deformation, the pore-struts bends and a deformation band is generated, which is perpendicular or tilted to the load-direction. Finally, the pores collapse.

Fig. 4. Factors influencing energy absorption efficiency: (a) strain rate, (b) porosity, and (c) pore size.

absorption ability. Furthermore, when the strain rate and porosity are constant, it can be concluded that OCCF with larger pore size has greater energy absorption ability. Obviously, a majority of energy absorption efficiency of the specimens are

Table 2. Plastic hardening parameters.

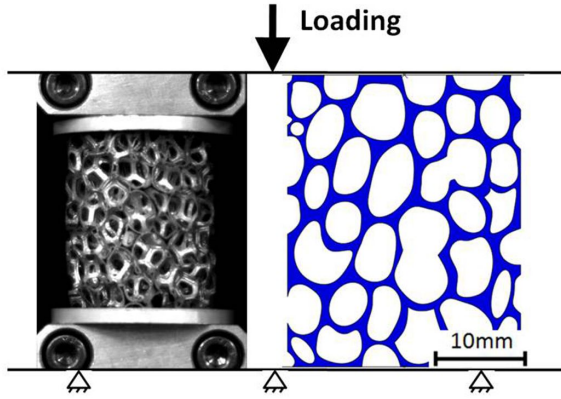| Yield stress [MPa]	2.00	2.73	3.38	3.78	4.87	5.54	6.36	7.36	8.85
Plastic strain	0	0.04	0.13	0.17	0.22	0.29	0.32	0.36	0.39

Fig. 5. Loading mode for test and simulation.

With further compression, deformation bands combine together, OCCFs collapse and densify by the layer-by-layer collapsing. Moreover, area A and B in Fig. 6 show that when the stress surpasses the yield strength of the foam material, a local stress concentration is observed. The stress concentrates at the weak pore-struts with a tiny deformation, where the energy absorption is less. When the strain reaches the value of 25 %, most of the pores gradually collapse and a few pores collapse completely. The plastic deformation increases dramatically at the weak pore-struts but it increases at the strong pore-struts. A large amount of energy is absorbed by OCCF during the deformation.

Relative errors for Young modulus, yield strength as well as compressive strength between the simulations and tests are shown in Table 2, and they are 5.9 %, 6.3 % and 4.6 %, respectively. It means that the two-dimensional random model is suitable for simulating the mechanism of energy absorption under uniaxial compression. The stress-strain curves for a whole specimen and area A and B in Fig. 6 are shown in Fig. 7. When the strain reaches 0.1, the stress at area A increases
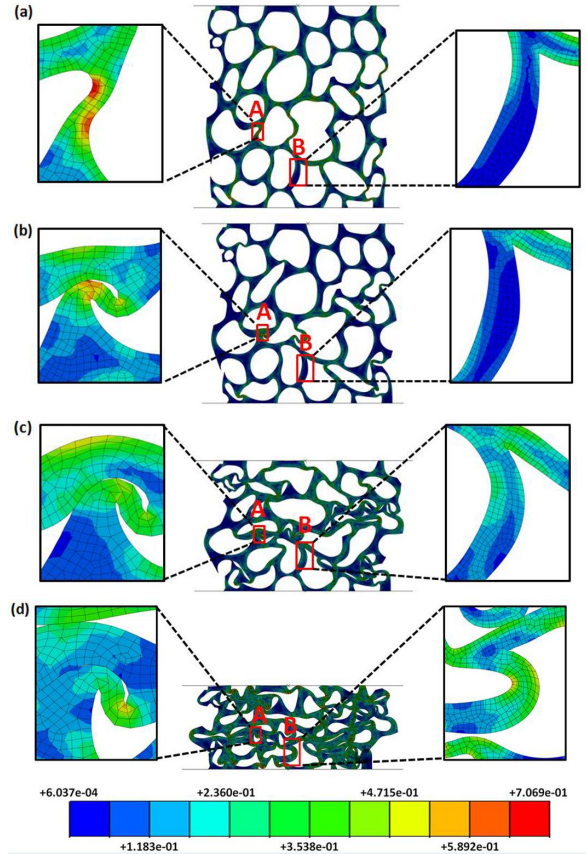

Fig. 6. The nephograms for von Mises stress of copper foam: a) $\epsilon = 3$ %, (b) $\epsilon = 10$ %, (c) $\epsilon = 25$ %, (d) $\epsilon = 45$ %

significantly and is larger than the stress for the whole specimen while the stress at area B is smaller than the stress for the whole specimen. This phenomenon illustrates that it is easy to generate the permanent plastic deformation - the main factor affecting the energy absorption at the weak pore-struts during the simulation, which coincides with the experimental results.
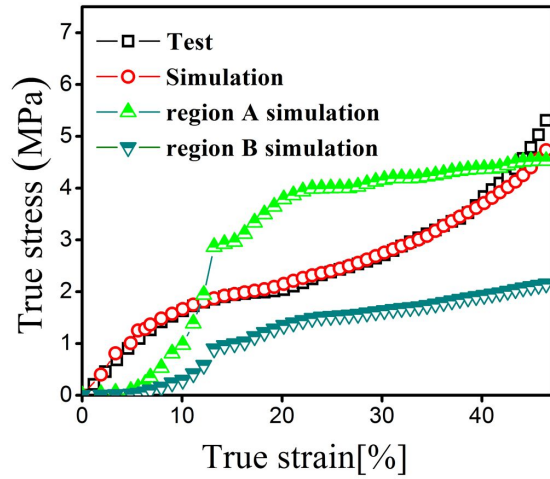
Fig. 7. The comparison of simulation curve and test curve.

Table 3. Characteristic parameters relative error of test and simulation.

Parameter [MPa]	Trail curve	Simulated curve	Relative error [%]
Young modulus E	29.83	31.59	5.9
Yield stress σ_y	1.90	2.02	6.3
Compressive strength σ_c	2.83	2.96	4.6

4. Conclusions

1. There are elastic stage, plastic stage and densification stage in the true stress-strain curve of OCCF, and the compressive strength, Young modulus and yield stress increase with increasing strain rate and decreasing porosity and pore size.

2. Energy absorption efficiency of OCCF with high porosity is higher than 65 %, and the highest efficiency is observed when the strain is between 0.2 and 0.3. Increasing porosity and decreasing pore size improve the energy absorption efficiency.

3. The relative error of Young modulus, yield stress as well as compressive strength between simulations and tests is 4.1 %, 9.8 % and 3.2 %, respectively. It shows that energy

absorption process under uniaxial compression can be predicted by two-dimensional random model. The permanent plastic deformation is easy to generate at the weak pore-struts, which is the main factor affecting the energy absorption.

References

[1] Chiang Y. M., *Science*, 330(2010), 1485.
[2] Kalnausa S., Rhodes K., Daniel C., *J. Power Sources*, 196 (2011), 8116.
[3] Liang B., Liu Y.P., Xu Y.H., *J. Power Sources*, 267 (2014), 469.
[4] Xie W., Zhu X.K., Yi S.H., Kuang J.C., Cheng H.F., *Mater. Des.*, 90 (2016), 38.
[5] Wu X.W., Li Y.H., Li C.C., He Z.X., Xiang Y.H., *J. Power Sources*, 300 (2015), 453.
[6] Chen J.L., Chen J., Chen D., Zhou Y., Li W., *Mater. Lett.*, 117 (2014), 162.
[7] Li W., Chen J., Liang H., Li C., *Mater. Sci.*, 33 (2015), 356.
[8] Yao M., Okuno K., Iwaki T., Awazu T., Sakai T., *J. Power Sources*, 195 (2010), 2077.
[9] Baggetto L., Verhaegh N.A.M., Niessen R.A.H., Roozeboom F., Jumas J.C., Notten P.H.L., *J. Electrochem. Soc.*, 157 (2010), 340.
[10] Chou C.Y., Kim H., Hwang G.S., *J. Phys. Chem. C*, 115 (2011), 20018.
[11] McDowell M. T., Lee S.W., Wang C.M., Cui Y., *Nano Energy*, 1 (2012), 401.
[12] Nguyen C.C., Song S.W., *Electrochim. Acta*, 55 (2010), 3026.
[13] Beaulieu L.Y., Beattie S.D., Hatcharda T.D., Dahn J.R., *J. Electrochem. Soc.*, 150 (2003), 419.
[14] Bogart T.D., Chockla A.M., Korgel B.A., *Curr. Opin. Chem. Eng.*, 2 (2013), 286.
[15] Jiang T., Zhang S.C., Qiu X.P., Zhu W.T, Chen L.Q., *J. Power Sources*, 166 (2007), 503.
[16] Huang L., Cai J.S., He Y., Ke F. S., Sun S.G., *Electrochem. Commun.*, 11 (2009), 950.
[17] Ke F.S., Huang L., Wei H.B., Cai J.S., Fan X.Y., Yang F.Z., Sun S.G., *J. Power Sources*, 170 (2007), 450.
[18] Ke F.S., Huang L., Cai J.S., Sun S.G., *Electrochim. Acta*, 52(2007), 6741.
[19] Shin H.C., Liu M., *Adv. Funct. Mater.*, 15 (2005), 582.
[20] Arbizzani C., Beninati M., Lazzari M., Mastragostino M., *J. Power Sources*, 158 (2006), 635.

[21] ZHAO H.P., JIANG C.Y., HE X.M., REN J.G., WAN C.R., *J. Membr. Sci.*, 310 (2008), 1.

[22] IONICA B.C.M., LIPPENS P.E., ALDON L., OLIVIER F.J., JUMAS J.C., *Chem. Mater.*, 18 (2006), 6442.

[23] QIN F., ZHANG J.H., ZHANG Y.D., LIU J.C., GONG Z.M., *Compos. Struct.*, 124 (2015), 409.

[24] JUNG A., BEEX L.A.A., DIEBELS S., BORDAS S.P.A., *Mater. Des.*, 87 (2015), 36.

[25] SUN Y., RIGOBERTO B., VANDERKLOK A. J., TEKALUR S. A., WANG W., LEE I., *Mater. Sci. Eng. A-Adv.*, 592 (2014), 111.

[26] RAJAK D.K., KUMARASWAMIDHAS L.A., DAS S., KUMARAN S.S., *J. Alloy. Compd.*, 656 (2016), 218.

[27] ZUMAN P., *Microchem J.*, 75(2003), 139.